Emergent Berezinskii-Kosterlitz-Thouless Phase in Low-Dimensional Ferroelectrics

Y. Nahas,[1,*] S. Prokhorenko,[1,2] I. Kornev,[3] and L. Bellaiche[1]

[1]*Physics Department and Institute for Nanoscience and Engineering, University of Arkansas, Fayetteville, Arkansas 72701, USA*
[2]*Theoretical Materials Physics, Q-MAT CESAM, Université de Liège, B-4000 Sart Tilman, Belgium*
[3]*Laboratoire Structures, Propriétés et Modélisation des Solides, CentraleSupélec, 92290 Châtenay-Malabry, France*

Using first-principles-based simulations merging an effective Hamiltonian scheme with scaling, symmetry, and topological arguments, we find that an overlooked Berezinskii-Kosterlitz-Thouless (BKT) phase sustained by quasicontinuous symmetry emerges between the ferroelectric phase and the paraelectric one of $BaTiO_3$ ultrathin film, being under tensile strain. Not only do these results provide an extension of BKT physics to the field of ferroelectrics, but they also unveil their nontrivial critical behavior in low dimensions.

In two-dimensional systems with continuous symmetry and short-range interactions, strong fluctuations prevent the formation of long-range order [1,2], and rather than a spontaneous symmetry breaking, a topological phase transition driven by the unbinding of vortex-antivortex pairs can occur, the so-called Berezinskii-Kosterlitz-Thouless (BKT) transition [3,4]. It is an infinite-order phase transition [5] and is paradigmatically captured by the two-dimensional XY model that has attracted much interest for it astutely describes, amongst others, the physics of superfluid helium films [6], superconducting films [7–9], the Coulomb gas model [10], Josephson junction arrays [11], and nematic liquid crystals [12]. Ferroelectrics on the other hand, which constitute an important class of materials, are *prima facie* not expected to exhibit BKT transition, owing to their discrete symmetry stemming from the cubic anisotropy of both the lattice and the ferroelectric interactions, which include the long-range dipolar ones. Whether the BKT behavior would be robust against the introduction of symmetry-breaking ferroelectric anisotropy remains unsettled. Here we show, using Monte Carlo simulations of a first-principles-based effective Hamiltonian scheme as well as scaling, symmetry, and topological arguments, that an intermediate critical BKT phase underlain by quasicontinuous symmetry emerges between the ferroelectric phase and the disordered paraelectric one in tensily strained thin film of $BaTiO_3$, a prototypical ferroelectric. We find that this overlooked intermediate phase supports quasilong-range order reflected in the algebraic decay of the correlation function and sustained by the existence of neutral bound pairs of vortices and antivortices, in accordance with defining characteristics of a BKT phase. Its lower and upper critical temperatures, T_c and T_{BKT}, are associated with the condensation and unbinding of vortex-antivortex pairs, respectively. Moreover, we also find that upon reaching T_{BKT}, the correlation function's critical exponent acquires a value

close to the theoretical predictions 0.25 of the XY model [3,4], further indicating that the upper transition is likely to be of the BKT type. Our results therefore highlight the subtle, fundamental richness of low-dimensional ferroelectrics and widen the realm of BKT transitions.

The situation described by the highly idealized two-dimensional XY model [3,4] conventionally only applies to two-dimensional degenerate systems with local interaction, and is scarcely met in experiments involving ferromagnetic and ferroelectric systems. In these systems, the presence of a dipole-dipole interaction, nonlocal in nature, significantly reduces fluctuations, thereby altering the low-temperature properties of the XY model [13]. Indeed, it is well known that the dipolar interaction tends to stabilize the long-range order against thermal fluctuations, and the ground state may thus be spontaneously polarized [14,15], or acquire various structures. However, while the low-temperature properties substantially depend on the dipolar interaction, in the high-temperature regime this interaction is of a lesser significance [16], and its contribution demonstrated to be irrelevant in the treatment of the dipolar XY model [13,15–18]. Furthermore, in an anisotropic variant of the two-dimensional XY model with short-range interactions [19,20], it was found that the introduction of a small effective anisotropy had no effect in altering the BKT transition. Hence there appears to be a breach for investigating ferroelectrics such as barium titanate, wherein there exists a natural propensity for disorder, reflected for instance in the order-disorder component of its phase transition [21,22]. The easy displacement of titanium ions from the centrosymmetric position, occurring even in the cubic phase, along the degenerate rhombohedral low-symmetry directions renders its higher-symmetry tetragonal and orthorhombic ferroelectric phases only partially ordered [21,23], i.e., still subject to fluctuations. In reduced dimensionality, one may thus inquire whether the interplay between the geometrical enhancement of these intrinsic

fluctuations and its necessary alteration by anisotropy and long-range dipolar interactions would allow for a subtle manifestation of BKT physics in ferroelectric thin films (see the section "Mixed order-disorder/displacive behaviors and associated precursor effects" in Supplemental Material [24]).

During the past decade, the physical properties of thin ferroelectric films have been the subject of intense investigation, in part due to the prospect of using such films in microelectronics, such as nonvolatile random access memories [40], but also due to their novel and unique physical properties that single them out from their three-dimensional counterparts. Recent experimental developments have brought low-dimensional ferroelectric systems within reach in laboratory, thereby rendering them particularly interesting for exploring new phenomena, addressing fundamental questions, and testing the reliability of numerical predictions. In order to gain insight into their critical properties, we simulate thin films made of $BaTiO_3$ under open-circuit electrical boundary conditions, grown along the [001] pseudocubic direction (chosen to be the z axis), and Ba-O terminated. Such films are mimicked by $L \times L \times h$ supercells that are periodic along the x and y axes (which lie along the [100] and [010] pseudocubic directions, respectively), and finite along the z axis (which corresponds to the [001] direction). We consider a thickness h of three unit cells corresponding to 11.7 Å, and investigate several lateral sizes of $L = \{24, 26, 28, 30\}$ unit cells. We subject the film to tensile strain (∼3%) mimicking the effect of a substrate with a notably larger lattice parameter. Interestingly, anisotropically stressed perovskite crystals are known to exhibit phase diagrams with interesting complexities and can display a variety of types of critical behavior [41,42]. The considered supercell is depicted in Fig. 1(a). The total energy of the film, used to predict its properties through extensive Monte Carlo simulations over at least 14×10^6 sweeps, is described in the methods section of Supplemental Material [24].

In Fig. 1(b), we show the distribution of local dipole Cartesian components at 25 K within a $30 \times 30 \times 3$ supercell. It is therein seen that due to strong tensile strain, local dipole moments are confined to the film plane, and thus polarization can be regarded as a two-component order parameter. Note that the macroscopic spontaneous polarization is numerically found to lie along a ⟨110⟩ pseudocubic direction for any temperature below the Curie point of 539 K. Calculating the contribution of the interplane coupling to the total energy of the system, we find that it does not exceed 4%. Therefore, due to the weak interplane coupling, dipoles belonging to different planes are uncorrelated and the investigated ultrathin film geometry can be considered as effectively two dimensional. The assessment of the order of the ferroelectric phase transition in tensily strained $BaTiO_3$ thin film is conducted using the Wang-Landau algorithm [43,44], which enables accessing the
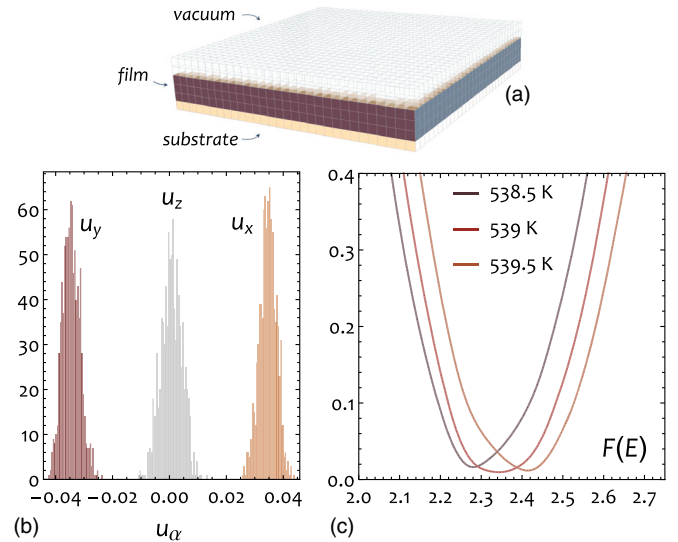
FIG. 1. (a) Schematic view of the considered supercell. (b) Distribution of local dipole components at 25 K for $30 \times 30 \times 3$ $BaTiO_3$ thin film under 3% tensile strain. (c) Free-energylike quantity versus internal energy (in Hartree) of the $30 \times 30 \times 3$ $BaTiO_3$ supercell under 3% tensile strain at and around T_C.

density of states from which a free-energylike quantity can be calculated. While for discontinuous phase transitions, the free energy F versus the internal energy E features a double-well structure, at criticality and for continuous transitions, only a single minimum is present. Figure 1(c) indicates that the considered $BaTiO_3$ system falls in the latter case in vicinity of the Curie point, in accordance with Landau theory [45], and with allowance for scaling analysis [20]. Invoking finite-size scaling arguments enables the determination of the extent of the intermediate critical BKT phase that we find ranging between $T_c \sim 539$ K and an upper critical temperature, $T_{BKT} \sim 545$ K (see the section "Scaling analysis and intermediate critical phase" in Supplemental Material [24]).

One of the features mirroring the uniqueness of the BKT phase lies in the quasilong-range order it can sustain. This quasilong-range ordered phase is characterized by the slow algebraic decay of the order parameter correlation function and its continuously varying critical exponent η [4,20]. This algebraic behavior is similar to that of an isolated critical point while not being confined to a single temperature, and the BKT phase can thus be regarded as a phase consisting of critical points, distinct from the high-temperature disordered phase with rapid exponential decay of the correlation function, yet weaker than a truly long-range ordered one. From BKT theory [4], it is expected that quasilong-range order onsets at T_{BKT} and that it is marked by $\eta(T_{BKT}) = 0.25$. We therefore inquire into the behavior of the in-plane two-point disconnected correlation function [46] in the considered $BaTiO_3$ system. Results indicate that within the identified intermediate phase, the correlation function is best fitted into a power-law falloff [inset of Fig. 2(a)], while for higher temperatures, it is the

(a)

(b)
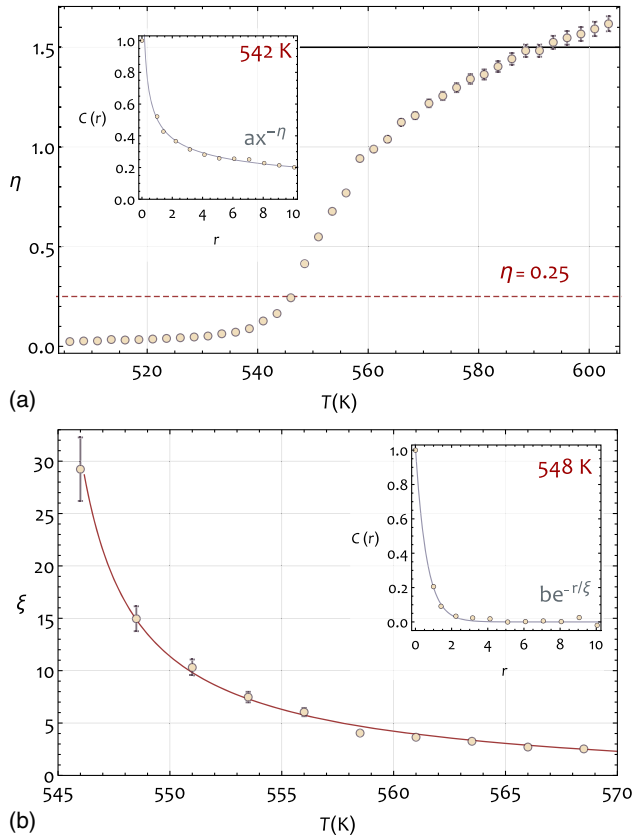
FIG. 2. Evolution with temperature, for $L = 30$, of the in-plane two-point correlation function exponent η (a) and the correlation length ξ (b) as determined from fit to spatial correlation with power and exponential laws, exemplified by the insets of (a) and (b), respectively. The red line in (b) corresponds to an exponential fit to the data points.

exponential form that best captures the rapid decay of the correlation, as is typical of a disordered, paraelectric phase [inset of Fig. 2(b)]. Extracting the values of η and ξ from power-law and exponential fits to the disconnected correlation function, we obtain an estimate of their temperature dependence. It is seen in Fig. 2(a) that the temperature at which the predicted 0.25 value of the critical exponent η of the correlation function is reached falls in close vicinity of the previously estimated $T_{BKT} \sim 545$ K, in agreement with the BKT picture [4] (see the "Scaling analysis and intermediate critical phase" section in Supplemental Material [24]). Moreover, as shown in Fig. 2(b), the expected exponential divergence of the correlation length ξ upon reaching BKT from above [4] is indeed observed in our simulations.

The above gathered results entail the existence of an intermediate critical BKT phase in tensily strained BaTiO$_3$ thin film, separating the ferroelectric phase from the disordered one, and characterized by quasilong-range order and the absence of symmetry breakdown. The three-phase structure exhibited by the considered dipolar system can be further qualitatively evidenced through the consideration of
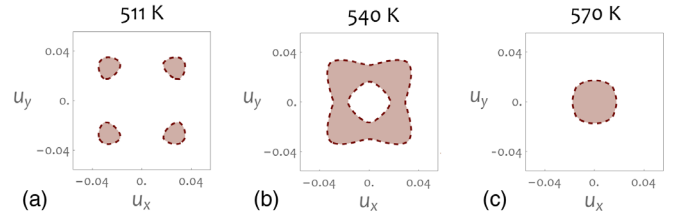
FIG. 3. Temperature evolution of the symmetrized probability distribution of the in-plane components of local dipole moments in a $L = 30$ supercell.

dipolar fluctuations, whose role is exacerbated by the reduced dimensionality. Figure 3 shows the symmetrized probability distribution of local dipole moments [47] and points to three phases with distinct topologies. Upon decreasing temperature, the system transits from a uniform distribution around 0, characteristic of a disordered state at high temperatures [Fig. 3(c)], to four isolated spots, indicative of a fourfold-degenerate ground state [Fig. 3(a)], through an approximate continuous rotational symmetry reflected in a nearly annular distribution at intermediate temperatures [Fig. 3(b)]. In this intermediate regime, dipoles acquire nonzero magnitude while retaining their fluctuations, yielding a distribution with ring topology whose slight distortion reflects the anisotropy of the underlying square lattice. Hence, while the critical behavior is usually determined by the range of interactions, spatial dimensionality, and inherent symmetry of the Hamiltonian, in some cases such as the one considered here, at criticality, a higher, quasicontinuous symmetry of the discrete order parameter can arise, rendering the associated critical behavior richer than expected [48,49]. Indeed, while the fourfold anisotropy is relatively irrelevant in the intermediate critical BKT phase where the two-dimensional XY model properties are recovered and an approximate continuous symmetry is observed, it reasserts itself suppressing fluctuations and restoring the fourfold rotational symmetry at low temperatures. It is primarily interesting to note that this critical phase with emergent continuous symmetry is reminiscent of the intermediate BKT phase between the low-temperature ordered phase and the high-temperature disordered phase of the square planar rotator model with small fourfold symmetry-breaking field [50] (see the section "Interplay between isotropy and anisotropy" in Supplemental Material [24]).

A salient feature of the BKT transition is its intricate relation with topological excitations, namely, vortices and antivortices point defects [4]. The seminal heuristic argument of Kosterlitz and Thouless points to a subtle logarithmic competition between energy and entropy of defects, the balance point of which, marked by T_{BKT}, insulates two different modes of their behavior [4]. Below this transition temperature, lone defects are inhibited due to their logarithmically divergent energy with the system size, and hence vortices or antivortices are expected not to occur in isolated form, but rather within tightly bound vortex-antivortex pairs

as local excitations, due to the finite pair energy scaling with its radius rather than with the system size. These bound pairs appear topologically neutral from a large-scale perspective, as they confine and mutually cancel their orientational disturbance, thereby allowing for algebraic decay of correlations and quasilong-range order. As temperature is raised, the number of pairs increases and larger ones start forming, within which the interaction of defects is subject to screening by other smaller pairs that lie in between. These loosened pairs effectively unbind at T_{BKT}, whereupon entropy balances the interaction and independent free defects occur, causing correlations to decay exponentially in the high-temperature phase. The relevance of defects in establishing the BKT transition is hence crucial, and their very existence anchors in the nontriviality of the fundamental homotopy group (π_1) of the underlying circle topology (S^1 of the XY-model symmetry group, $\pi_1(S^1) = \mathbb{Z}$, where $\mathbb{Z}$ is the group of integers). On a lattice, such defects can thus be identified through a topological invariant or discrete winding number $k \in \mathbb{Z}$ [51,52], measuring the accumulated angular variation of vectors upon circulating with a given orientation along elementary plaquettes composing the square lattice. Whenever vectors process by $+2\pi$ (-2π), the plaquette encloses a vortex (antivortex) with $k = +1$ ($k = -1$). Notably, the topology of the emergent quasicontinuous symmetry exhibited by tensily strained BaTiO$_3$ thin film at intermediate temperatures [Fig. 3(b)] is topologically equivalent, or homeomorphic, to the circle S^1 topology underlying the O(2) symmetry group of the XY model, hence endowing defects with topological protection against simple perturbations in the considered system [53]. We thus undertake the examination of the behavior of defects by characterizing the topological properties of the two-dimensional cross-sectional polarization field. We find that while such defects are absent deep in the ferroelectric phase, they condensate in close vicinity of T_c in the form of strongly coupled vortex-antivortex pairs [Fig. 4(a1)], marking the breakdown of long-range order, and the accommodation of quasilong-range ordering instead. Indeed, winding numbers are additive, and the two oppositely charged defects within pairs compensate each other, such that the resulting texture can be immersed in a uniform background, yielding a power-law decay of dipolar correlations [inset of Fig. 2(a)]. We note that while the existence of an odd number of vortices or antivortices is prohibited by the condition of zero overall vorticity at stake in the considered system with periodic boundary conditions, the generation by thermal fluctuations of such pairs is both allowed topologically and favored energetically by short-range interactions between first and second nearest neighbors. The mean vortex-antivortex separation within a pair, or pair radius r, is found not to exceed around one lattice spacing and is significantly smaller than the mean separation between pairs [Fig. 4(a1)]. As T_{BKT} is approached from below, the number of pairs increases, and loosely bound pairs start occurring
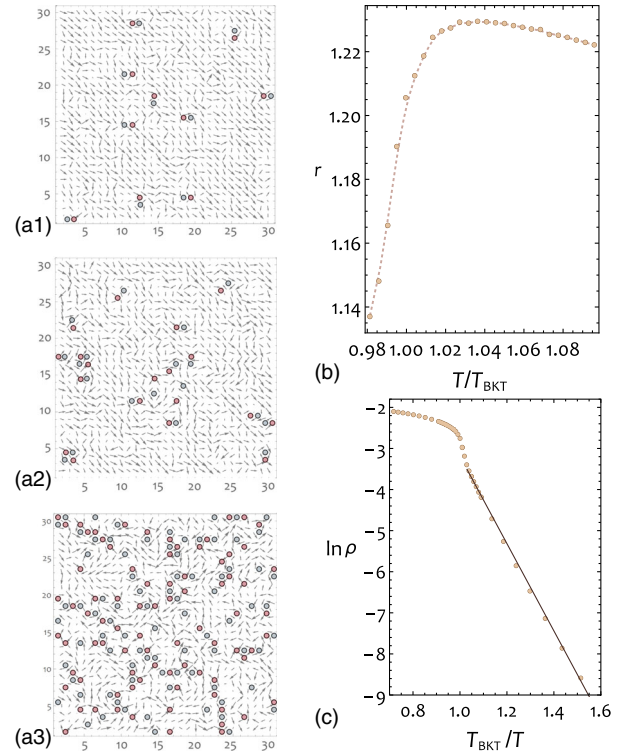
FIG. 4.   (a) Spatial distribution of vortices (blue points) and antivortices (red points) overlaid on cross-sectional dipolar configuration for $L = 30$ at (a1) 540 (intermediate BKT phase), (a2) 545 ($\sim T_{BKT}$), and (a3) 550 K (paraelectric phase). (b) Evolution of the average vortex-antivortex pair radius r with reduced temperature T/T_{BKT}. The dashed curve is a guide for the eye. (c) Evolution of the logarithm of the average vortex-antivortex pairs density ρ with the inverse reduced temperature. The straight line is the linear fit to low-temperature data.

[Fig. 4(a2)]. Ensuingly, an unbinding onsets just above T_{BKT}, whereupon pairs with radius comparable to the mean separation between pairs begin to appear [Fig. 4(a3)]. This preliminary insight signals proliferation and unbinding of pairs as T increases through T_{BKT}, and is in qualitative agreement with the BKT picture [4,54]. To better support these observations, we examine the defect configurations and compute the evolution with temperature of the average vortex-antivortex pair radius r [Fig. 4(b)]. We find that r grows rapidly as T increases, which confirms the unbinding of vortex-antivortex pairs. At higher temperature, the curve decreases due to defects proliferation, which raises the probability of a defect having a neighboring antidefect. We next inquire into the temperature dependence of the density ρ of pairs, and find that bound vortex-antivortex pairs are concomitant with low defect concentration. In the corresponding temperature regime, the density of pairs is expected to be governed by a Boltzmann factor involving the chemical potential 2μ of a vortex-antivortex pair, $\rho \sim \exp[-2\mu/(T/T_{BKT})]$. Figure 4(c) shows $\ln \rho$ versus the inverse reduced temperature. As can be seen for low temperatures, $\ln \rho$ is proportional to T_{BKT}/T with the slope

being -10.49 ± 0.01, which is remarkably close to the value of $2\mu = 10.2$ that is expected for creating a vortex-antivortex pair of defects separated by unit distance in the continuum limit [4] in the BKT phase. The agreement between our obtained chemical potential in the dilute limit [Fig. 4(c)], which conditions the probability of appearance of a vortex-antivortex pair, and that predicted for the two-dimensional XY model can be apprehended through the fact that the contribution of the dipolar interaction, despite its seeming potential importance, has been analytically demonstrated to be irrelevant to the nature of the BKT transition within a dipolar variant of the XY model [16–18], in which the characteristic logarithmic interaction of defects within a pair was shown to be restored. While large chemical potential supports a dilute phase of defect pairs, one can see that for higher temperatures the slope significantly decreases, indicating smaller chemical potential, as it becomes thermally easier to create very many pairs (the presence of which decreases the free energy by increasing the entropy), leading to increased screening and effective dissociation upon reaching the paraelectric phase.

In summary, our numerical simulations provide evidence for an additional intermediate BKT phase in tensily strained BaTiO$_3$ thin film. We find that, due to an effectively reduced spatial dimensionality and a lessened number of dominantly contributing polarization components, the transitional region of tensily strained BaTiO$_3$ is enhanced into a critical phase exhibiting defining BKT features. In contrast with short-range isotropic systems, the anisotropic dipolar interactions ineluctably drive ferroelectric long-range order, thereby endowing the system with a three-phase structure: a truly ordered ferroelectric phase, a quasilong-range ordered phase substantiated by an algebraic decay of spatial correlations and supported by an emergent continuous symmetry that allows for stable topological excitations to condense in the distortion-confining form of vortex-antivortex bound pairs, and a disordered, paraelectric one, with exponentially falling correlations.

*yousra.nahas@gmail.com

[1] N. D. Mermin and H. Wagner, Phys. Rev. Lett. **17**, 1133 (1966).

[2] P. C. Hohenberg, Phys. Rev. **158**, 383 (1967).

[3] V. L. Berezinskii, ZhETF **61**, 1144 (1972) [Sov. Phys. JETP **34**, 610 (1972)].

[4] J. M. Kosterlitz and D. J. Thouless, J. Phys. C **6**, 1181 (1973).

[5] *40 Years of Berezinskii-Kosterlitz-Thouless Theory*, edited by J. V. José (World Scientific Publishing Co. Pte. Ltd., Singapore, 2013).

[6] D. J. Bishop and J. D. Reppy, Phys. Rev. Lett. **40**, 1727 (1978).

[7] M. R. Beasley, J. E. Mooij, and T. P. Orlando, Phys. Rev. Lett. **42**, 1165 (1979).

[8] A. F. Hebard and A. T. Fiory, Phys. Rev. Lett. **44**, 291 (1980).

[9] S. A. Wolf, D. U. Gubser, W. W. Fuller, J. C. Garland, and R. S. Newrock, Phys. Rev. Lett. **47**, 1071 (1981).

[10] J. Frohlich and T. Spencer, Commun. Math. Phys. **81**, 527 (1981).

[11] D. J. Resnick, J. C. Garland, J. T. Boyd, S. Shoemaker, and R. S. Newrock, Phys. Rev. Lett. **47**, 1542 (1981).

[12] P. E. Lammert, D. S. Rokhsar, and J. Toner, Phys. Rev. Lett. **70**, 1650 (1993).

[13] P. G. Maier and F. Schwabl, Condens. Matter Phys. **8**, 103 (2005).

[14] S. V. Maleev, ZhETF **70**, 2374 (1976) [Sov. Phys. JETP **43**, 1240 (1976)].

[15] P. G. Maier and F. Schwabl, Phys. Rev. B **70**, 134430 (2004).

[16] M. V. Feigel'man, ZhETF **76**, 784 (1979) [Sov. Phys. JETP **49**, 395 (1979)].

[17] P. O. Fedichev and L. I. Menshikov, Phys. Part. Nucl. Lett. **9**, 71 (2012).

[18] A. Y. Vasiliev, A. E. Tarkhov, L. I. Menshikov, P. O. Fedichev, and U. R. Fischer, New J. Phys. **16**, 053011 (2014).

[19] S. Miyashita, H. Nishimori, A. Kuroda, and M. Suzuki, Prog. Theor. Phys. **60**, 1669 (1978).

[20] K. Binder, Z. Phys. B **43**, 119 (1981); K. Binder, Phys. Rev. Lett. **47**, 693 (1981); K. Binder, M. Nauenberg, V. Privman, and A. P. Young, Phys. Rev. B **31**, 1498 (1985); K. Binder and D. W. Heermann, *Monte Carlo Simulations in Statistical Physics: An Introduction* (Springer-Verlag, New York, 1988); D. P. Landau and K. Binder, *A Guide to Monte Carlo Simulations in Statistical Physics* (Cambridge University Press, New York, 2005); *Application of the Monte Carlo Method in Statistical Physics*, edited by K. Binder (Springer-Verlag, Berlin, 1984).

[21] R. Blinc, Ferroelectrics **301**, 3 (2004).

[22] J. Hlinka, T. Ostapchuk, D. Nuzhnyy, J. Petzelt, P. Kuzel, C. Kadlec, P. Vanek, I. Ponomareva, and L. Bellaiche, Phys. Rev. Lett. **101**, 167402 (2008).

[23] R. Comes, M. Lambert, and A. Guinier, Solid State Commun. **6**, 715 (1968).

[24] See Supplemental Material http://link.aps.org/supplemental/10.1103/PhysRevLett.119.117601 for additional methodological information and discussions, which includes Refs. [25–39].

[25] L. Walizer, S. Lisenkov, and L. Bellaiche, Phys. Rev. B **73**, 144105 (2006).

[26] I. Ponomareva, I. I. Naumov, I. A. Kornev, H. Fu, and L. Bellaiche, Phys. Rev. B **72**, 140102R (2005).

[27] M. S. S. Challa and D. P. Landau, Phys. Rev. B **33**, 437 (1986).

[28] D. P. Landau, J. Magn. Magn. Mater. **31**–**34**, 1115 (1983).

[29] E. Almahmoud, I. A. Kornev, and L. Bellaiche, Phys. Rev. B **81**, 064105 (2010).

[30] A. M. Ferrenberg and R. H. Swendsen, Phys. Rev. Lett. **61**, 2635 (1988).

[31] D. Loison, J. Phys. Condens. Matter **11**, L401 (1999).

[32] M. E. Fisher, Rep. Prog. Phys. **30**, 615 (1967).

[33] A. Aharony and M. E. Fisher, Phys. Rev. B **8**, 3323 (1973).

[34] E. Almahmoud, I. A. Kornev, and L. Bellaiche, Phys. Rev. Lett. **102**, 105701 (2009).

[35] M. Stachiotti, A. Dobry, R. Migoni, and A. Bussmann-Holder, Phys. Rev. B **47**, 2473 (1993).

[36] T. Hidaka, J. Phys. Soc. Jpn. **61**, 1054 (1992).

[37] I. Ponomareva, L. Bellaiche, T. Ostapchuk, J. Hlinka, and J. Petzelt, Phys. Rev. B **77**, 012102 (2008).

[38] E. K. H. Salje, M. A. Carpenter, G. F. Nataf, G. Picht, K. Webber, J. Weerasinghe, S. Lisenkov, and L. Bellaiche, Phys. Rev. B **87**, 014106 (2013).

[39] J. Weerasinghe, L. Bellaiche, T. Ostapchuk, P. Kuel, C. Kadlec, S. Lisenkov, I. Ponomareva, and J. Hlinka, MRS Commun. **3**, 41 (2013).

[40] J. F. Scott, *Ferroelectric Memories* (Springer-Verlag, Berlin, 2000).

[41] A. Aharony and A. D. Bruce, Phys. Rev. Lett. **33**, 427 (1974).

[42] M. E. Fisher, Rev. Mod. Phys. **46**, 597 (1974).

[43] F. Wang and D. P. Landau, Phys. Rev. Lett. **86**, 2050 (2001).

[44] S. Bin-Omran, I. A. Kornev, and L. Bellaiche, Phys. Rev. B **93**, 014104 (2016).

[45] N. A. Pertsev, A. G. Zembilgotov, and A. K. Tagantsev, Phys. Rev. Lett. **80**, 1988 (1998).

[46] M. E. J. Newman and G. T. Barkema, *Monte Carlo Methods in Statistical Physics* (Oxford University Press, New York, 1999).

[47] S. Prokhorenko, Y. Nahas, and L. Bellaiche, Phys. Rev. Lett. **118**, 147601 (2017).

[48] J. V. José, L. P. Kadanoff, S. Kirkpatrick, and D. R. Nelson, Phys. Rev. B **16**, 1217 (1977).

[49] G. Ortiz, E. Cobanera, and Z. Nussinov, Nucl. Phys. **B854**, 780 (2012).

[50] E. Rastelli, S. Regina, and A. Tassi, Phys. Rev. B **70**, 174447 (2004).

[51] Y. Nahas, S. Prokhorenko, L. Louis, Z. Gui, I. A. Kornev, and L. Bellaiche, Nat. Commun. **6**, 8542 (2015).

[52] Y. Nahas, S. Prokhorenko, and L. Bellaiche, Phys. Rev. Lett. **116**, 117603 (2016).

[53] N. D. Mermin, Rev. Mod. Phys. **51**, 591 (1979).

[54] J. Tobochnik and G. V. Chester, Phys. Rev. B **20**, 3761 (1979).